# THE DISTRIBUTION OF PLUTONIUM-239 IN THE SKELETON OF THE MOUSE

D. Green, G.R. Howells, M.C. Thorne and J. Vennart
MRC Radiobiology Unit,
Harwell, Didcot, Oxon. OX11 ORD, U.K.

## 1. INTRODUCTION

It is well known that plutonium-239 is primarily deposited on the endosteal surfaces of cortical and trabecular bone and that after deposition it may either be resorbed, entering the reticuloendothelial system and blood, or buried under newly deposited bone mineral (1). However, the kinetics of these processes are not well understood. Such an understanding is of considerable importance in the field of radiological protection, since a knowledge of the detailed distribution of plutonium-239 in bone and its variation with time is necessary for the calculation of dose rates to those tissues thought to be at risk with respect to tumour induction (2), namely osteoprogenitor cells close to the endosteal surfaces of mineral bone and haematopoietic bone marrow (3).

In this paper we present some results from a detailed study of the distribution and retention of plutonium-239 in female CBA mice. This study which will cover the period 1 day to 18 months post-injection, is not yet complete and in this paper we present results only for animals killed at 24 hours post-injection. These results include radiochemical analyses of various bones together with analyses of the distribution of plutonium-239 in the central lumbar vertebra, a caudal vertebra and the ilium of each individual animal.

For the distribution studies we have used neutron induced autoradiography (4) together with computer based methods of data reduction. These techniques, which have been described in detail elsewhere (5), have allowed us to locate plutonium-239 with respect to bone surfaces with an accuracy of approximately $\pm$ 2μm.

It must be emphasised that these studies are of particular interest not only because of the information they should yield concerning the kinetics of plutonium-239 translocation in the skeleton but also because they should help with the interpretation of experiments on tumour induction performed in our laboratory (6) and elsewhere.

## 2. METHODS

Twelve week old female CBA mice were injected intravenously with 50nCi $kg^{-1}$ of plutonium-239-citrate at pH 4.5 and killed 24 hours later by exsanguination under chloroform anaesthesia. The bones to be analysed were then dissected out and, without prior decalcification processed through increasing concentrations of acetone and water prior to impregnation and embedding in resin. The embedded bone specimens were sectioned on a heavy-duty Jung microtome. The 5μm sections thus produced were floated off the knife, removed to a 60°C water bath to facilitate flattening and then to a 0.75mm Lexan (polycarbonate plastic) slide. The section was sandwiched between this Lexan slide and a second, similar, one. This assembly was held together with spring clips and dried at 60°C.

Lexan-bone preparations, prepared as described above, were sandwiched together in small packs and irradiated in a nuclear reactor at a neutron fluence of $10^{16}$ n $cm^{-2}$. The cadmium ratio of the neutron spectrum was 24, implying that more than 95% of the neutrons had energies of less than 0.5eV (7).

Following neutron irradiation the preparations were carefully separated and etched in 28% NaOH at 60°C for 75 minutes. The etched slides were then washed in tap water, rinsed in distilled water and air dried.

Neutron irradiation as described above induces two effects in the Lexan-bone preparations:

a plutonium-239 atoms in the section are fissioned by the neutrons and some of the fission fragments enter the Lexan producing damage tracks which can be etched out by NaOH

b the neutrons interact with the mineral bone in the section to produce an image of it in the Lexan. The mechanisms governing this process are still obscure although (n, $\alpha$) reactions may be implicated.

Examples of the high contrast bone images we are now obtaining routinely have been published elsewhere (5).

In order to obtain quantitative information from these bone and track images it is necessary to reduce the data contained in them to a numerical form. This we have done by analysing photographs of these images on D-MAC tables at the Rutherford Laboratory, Oxfordshire. These tables, normally used for the analysis of particle track photographs produced in high energy physics experiments, display a magnified image of the photographic negative ($\sim$50cm x 35 cm). The co-ordinates of any point on this image can be transferred to a magnetic tape by the movement of a cursor to the point of interest followed by a foot-pedal initiated data transfer. Additional information such as frame numbers and editing commands can be entered onto the tape from an alphanumeric keyboard.

Using these tables the edges of the bone image were digitised at intervals of about 1cm, corresponding to about 20$\mu$m on the original section. The co-ordinates of the ends of the fission fragment tracks were also digitised. It should be noted that no attempt was made to distinguish which end of a track represented its point of entry into the Lexan and that in the subsequent analysis both ends of each track were processed identically.

The magnetic tapes produced during digitisation were analysed on the IBM 370 computer at A.E.R.E. Harwell using programs developed by the authors. The primary purpose of these programs was to compute the quantities shown in figure 1, the perpendicular distances of track-ends from the bone image edge($X_1$ and $X_2$) and the angle of inclination of the tracks with respect to that edge ($\theta$). Measurement of this angle of inclination was useful, since tracks parallel to the bone image edge defined the perpendicular distance of their originating plutonium-239 atom from that edge more accurately than did tracks perpendicular to it. The greater significance of tracks parallel to the bone image edge was taken account of in the analysis by assigning a weight of $\cos^2\theta$ to each track-end when determining the distribution of track-ends about the bone image edge.

## 3. RESULTS

Figure 2 shows the distribution of weighted track-ends about the endosteal surfaces of the central lumbar vertebra at 24 hours post-injection. This distribution is centred close to the endosteal surface and the bulk of it lies within ± 15μm of that surface. However, this distribution is broader than the plutonium-239 distribution which gave rise to it, because of the finite distance the fission fragments travel in the section before entering the Lexan and because of the finite distance they travel in the Lexan before stopping. In order to correct for these effects a simple deconvolution analysis has been used.

The distribution of plutonium-239 about the bone image edge is approximated by 99 equally spaced planes, 1μm apart, parallel to the bone image edge and perpendicular to the plane of sectioning. The plutonium-239 concentration ($p_n$) associated with the n'th of these planes is proportional to the fraction of plutonium-239 between n-50.5 and n-49.5μm from the bone image edge, negative distances lying within the bone image. Similarly, the fraction of the weighted track end distribution between m-50.5 and m-49.5μm from the bone image edge is defined as $t_m$. The quantities $p_n$ and $t_m$ are related by;

$$t_m = \sum_n a_{mn} p_n \Big/ \sum_n p_n \qquad (1)$$

where $a_{mn}$ is the fraction of the weighted track-end distribution arising from $p_n$ that lies between m-50.5 and m-49.5μm from the bone image edge. Since the thickness of the specimen and the range of the fission fragments in bone and Lexan are known, $a_{mn}$ can be calculated for all values of m and n by computer based monte-carlo procedures.

Eqn. 1 can be expressed more concisely as;

$$\underset{\sim}{T} = \underset{\sim}{A}\,\underset{\sim}{P} \Big/ \sum_n p_n \qquad (2)$$

where $\underset{\sim}{T}$ and $\underset{\sim}{P}$ are 99 component vectors (i.e. both m and n range between 1 and 99) and $\underset{\sim}{A}$ is a 99 x 99 element square matrix. Thus, from Eqn. 2;

$$\underset{\sim}{P} / \Sigma p_n = \underset{\sim}{A}^{-1}\,\underset{\sim}{T} \qquad (3)$$

The matrix $\underset{\sim}{A}$ is, therefore, determined using monte-carlo procedures, inverted using sub-routine MA21B from the Harwell Sub-routine Library and multiplied by the observed track-end distribution to generate the plutonium-239 distribution which gave rise to it.

Results of this deconvolution analysis are shown in figures 3 and 4 for the 3 bones analysed so far. In figure 3 the distribution of plutonium-239 about the endosteal surfaces of these bones is shown. In the ilium the bulk of the plutonium-239 is very closely associated with the endosteal surfaces, whereas in the lumbar and caudal vertebræ there appears to be considerably more penetration of the plutonium-239 into the bone. This latter result is in general agreement with qualitative autoradiographic studies using plutonium-241 which show a rather broad distribution of plutonium in rat and hamster bone at early times post-injection together with significant uptake by osteogenic cells close to bone surfaces (N. Priest, Int. J. Radiat. Biol., in the press).

The narrowness of the plutonium-239 distribution about the endosteal surfaces of the ilium may be correlated with the gross morphology of the bone. The ilium contains a higher proportion of the cortical bone than do the lumbar and caudal vertebrae and this type of bone may be more difficult for the plutonium atoms to penetrate. Further analysis of the data so far obtained is being undertaken in order to check this possibility.

In contrast, figure 4 shows that the periosteal distribution of plutonium-239 is very similar in all three bones, suggesting that periosteal deposition is not strongly influenced by the type of bone under consideration. However, although the microscopic distribution is very similar in all three cases the concentration of track-ends associated with periosteal edges ($t_1$) is much higher in the caudal vertebra than it is in the other two bones (Table 1). Further, the concentration of track-ends associated with endosteal edges ($t_2$) is much lower in the caudal vertebra than it is in the other two bones (Table 1). These remarks, applying to observed bone image edges also apply, in three-dimensions, to the periosteal and endosteal surfaces of the bones. The two effects described above may be explained on the hypothesis that the blood supply to marrow is lower in the caudal vertebra than in the other two bones and that the periosteal blood supply is increased. This hypothesis is plausible, since it has been established that in mouse femur gross plutonium-239 deposition in various parts of the bone is well correlated with total blood flow in those regions (8).

In summary, a very satisfactory method has been developed for determining the distribution of plutonium-239 about bone surfaces. Results obtained so far indicate that plutonium is deposited primarily upon the endosteal surfaces of mineral bone, but not in a thin layer, there being considerable penetration of the mineral matrix probably via the lacunae even at 24 hours post-injection. Further, it has been demonstrated that the distribution of plutonium-239 about periosteal surfaces is, other than in absolute magnitude, rather independent of the bone considered. This indicates that factors such as blood supply are probably more important in governing the periosteal deposition of plutonium than is the detailed local structure of the periosteal surface.

REFERENCES


(1) VAUGHAN, J. in "Handbook of Experimental Pharmacology, 36, Uranium, Plutonium, Transplutonic Elements" Berlin, Springer Verlag pp 400-413 (1973)

(2) THORNE, M.C. Nature, Lond. 259 (1976) 539

(3) ICRP Publication 11 "A review of the radiosensitivity of the tissues in bone, Pergamon, Oxford (1968)

(4) JEE, W.S.S. "Plutonium-239 in bones as visualised by photographic and neutron-induced autoradiography" in Radiobiology of Plutonium (Stover, B.J. and Jee, W.S.S. Eds) J.W. Press, Salt Lake City, Utah (1972)

(5) GREEN, D., HOWELLS, G., THORNE, M.C. "A new method for the accurate localisation of plutonium-239 in bone", Phys. Med. Biol. (in the press)

(6) LOUTIT, J.F., SANSOM, Janet, CARR, T.E.F. "The pathology of tumours induced in Harwell mice by plutonium-239 and radium-226" in "The Health Effects of Plutonium and Radium" (Jee, W.S.S. Ed) J.W. Press, Salt Lake City, Utah (1976)

(7) IAEA "Neutron Fluence Measurements", STI/DOC/10/107 (Vienna, IAEA) pp 47-49 (1970)

(8) HUMPHREYS, E.R., FISHER, G. and THORNE, M.C. "The measurement of blood flow in mouse femur and its correlation with plutonium-239 deposition" (submitted to Calcified Tissue Research)

| Bone | f | $t_1$ | $t_2$ | C |
|---|---|---|---|---|
| Lumbar (1 + 2) | - | - | - | 113.6 ± 9.0 |
| Lumbar (3) | 0.150 ± 0.007 | 188 ± 24 | 841 ± 59 | - |
| Lumbar (4 + 5) | - | - | - | 119.4 ± 5.3 |
| Ilium | 0.138 ± 0.004 | 187 ± 14 | 824 ± 34 | 86.4 ± 1.8 |
| Caudal (Proximal) | - | - | - | 37.4 ± 1.6 |
| Caudal (Central) | 0.539 ± 0.012 | 333 ± 68 | 238 ± 28 | - |
| Caudal (Distal) | - | - | - | 58.2 ± 13.2 |

TABLE 1 Values describing the plutonium-239 distribution in various bones of the female CBA mouse at 24 hours post-injection.

f : Fraction of total track ends associated with periosteal edges.
$t_1$ : Concentration of track-ends associated with periosteal edges (track-ends/cm).
$t_2$ : Concentration of track-ends associated with endosteal edges (track-ends/cm)
C : Concentration of plutonium-239 in the whole bone (% Injected activity/g ash).

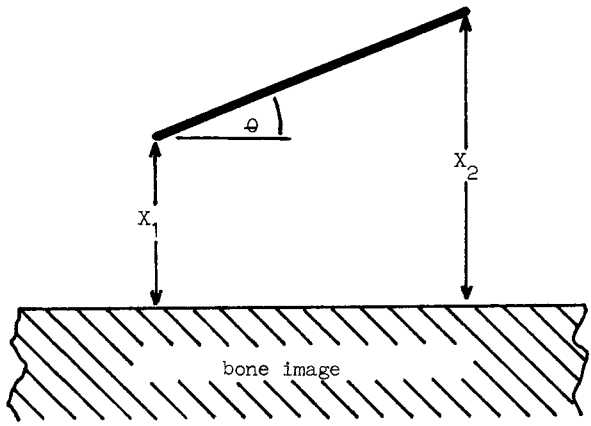


Figure 1. Quantities derived from the digitised data by the analysis programs.

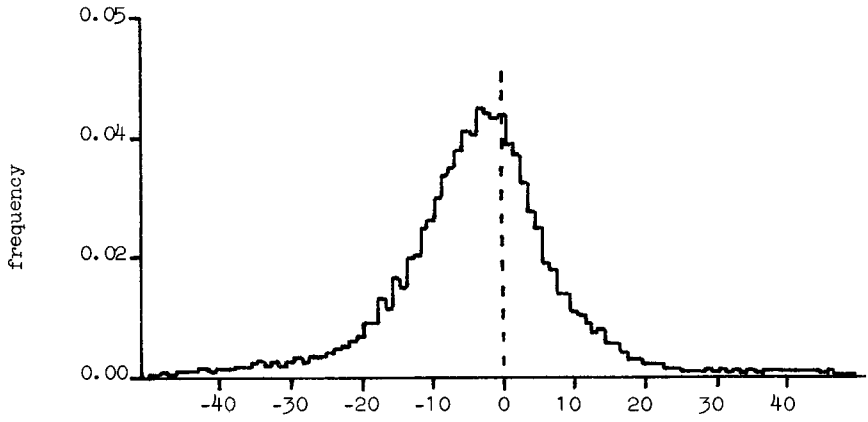


Figure 2. Weighted track-end distribution about the endosteal surfaces of the third lumbar vertebra at 24 hours post-injection. Negative distances are within the bone image.

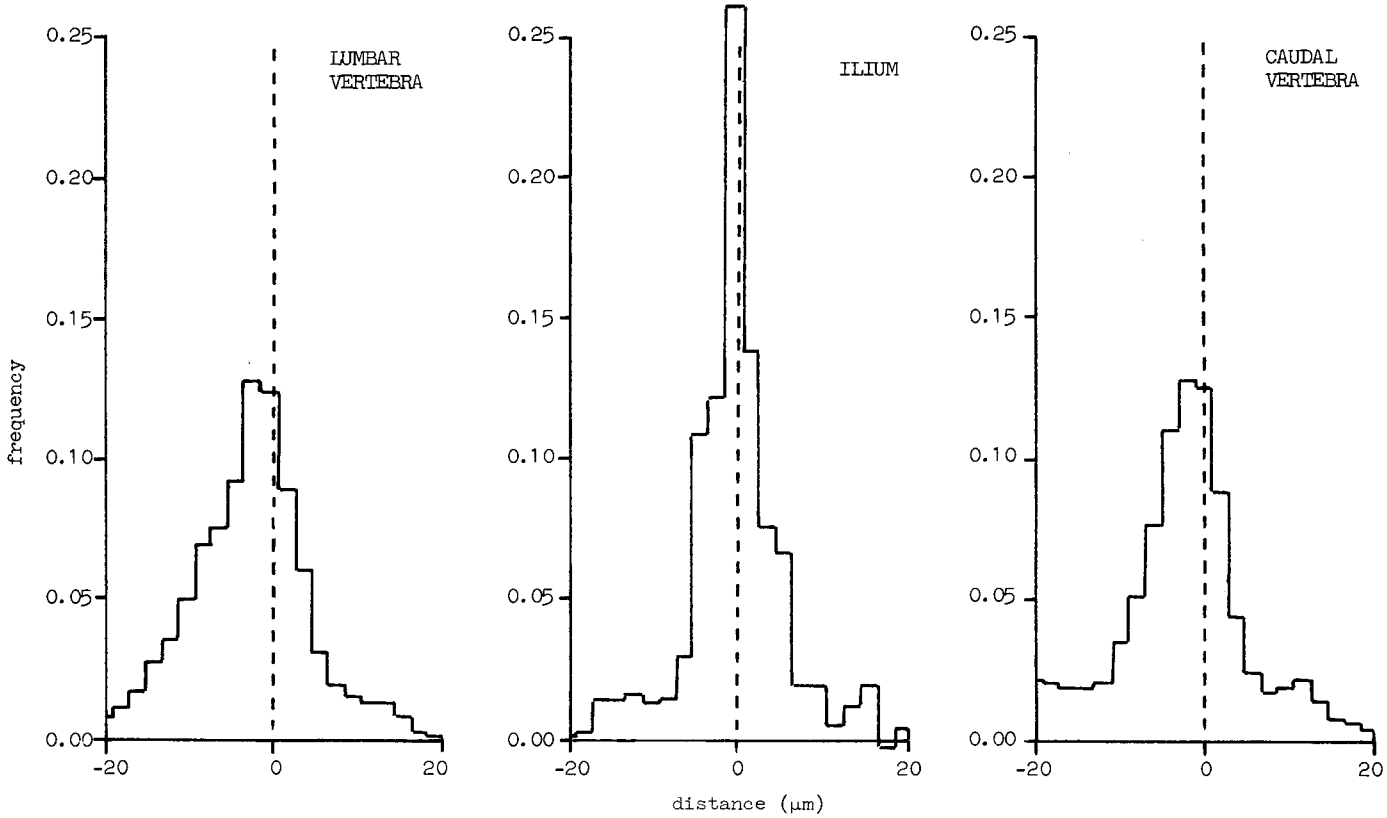


Figure 3. Plutonium-239 distributions about endosteal surfaces at 24 hours post-injection. Negative distances are within the bone image.

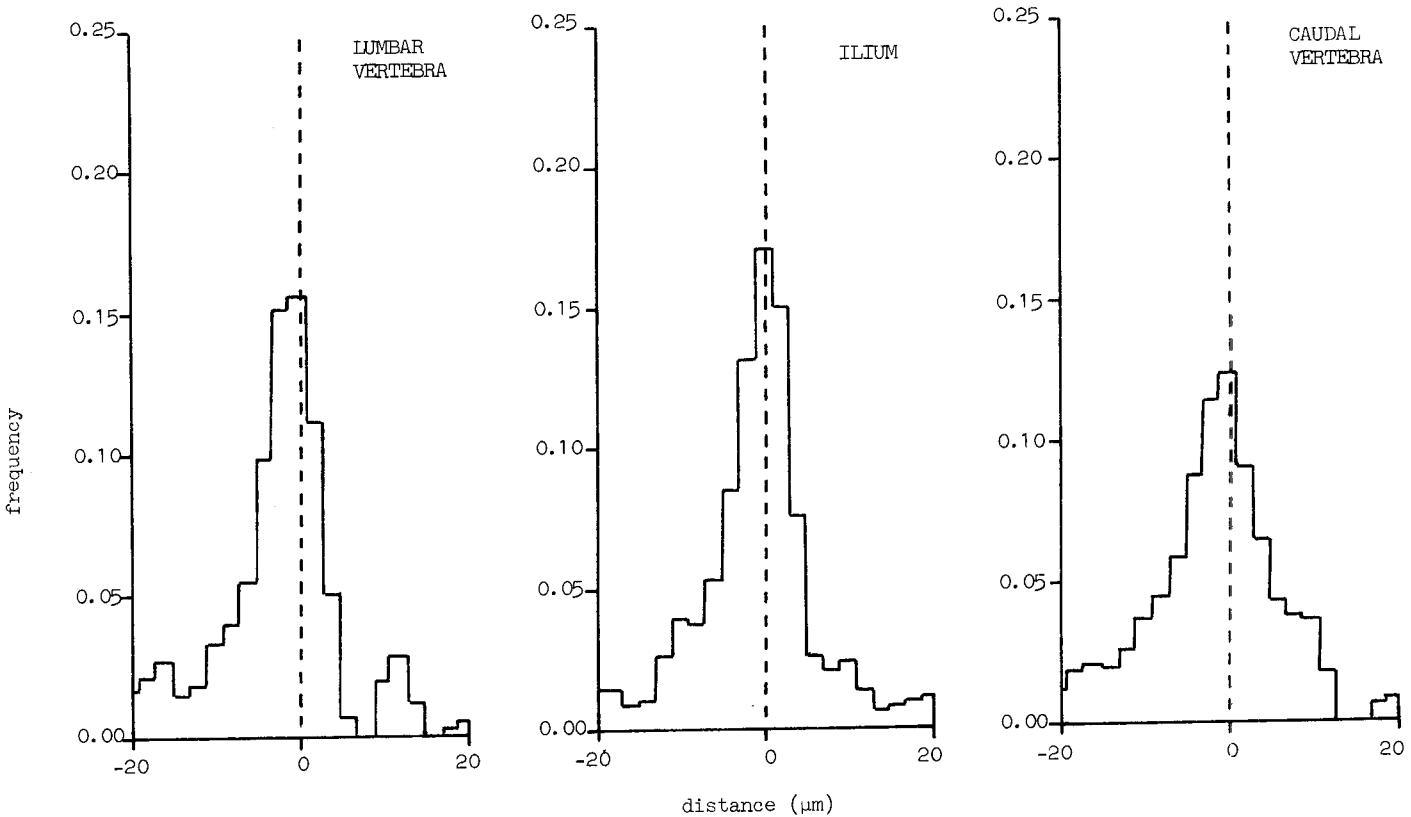


Figure 4. Plutonium-239 distributions about periosteal surfaces at 24 hours post-injection. Negative distances are within the bone image.